

Current Progress of a Finite Element Computational Fluid Dynamics Prediction of Flutter for the AeroStructures Test Wing

This progress report focuses on the use of the SStructural Analysis RoutineS suite program, *SOLIDS*, input for the AeroStructures Test Wing. The AeroStructures Test Wing project as a whole is described. The use of the *SOLIDS* code to find the mode shapes of a structure is discussed. The frequencies, and the structural dynamics to which they relate are examined. The results of the CFD predictions are compared to experimental data from a Ground Vibration Test.

Nomenclature

<i>CFD</i>	= Computational Fluid Dynamics
<i>ATW</i>	= AeroStructures Test Wing
<i>STARS</i>	= SStructural Analysis RoutineS
<i>GVT</i>	= Ground Vibration Test
<i>SOLIDS</i>	= Structural Solver
<i>FEM</i>	= Finite Element Method

Introduction

This project started as a result of a request from the NASA Dryden test center for a Computational Fluid Dynamics (CFD) prediction of the flutter boundary for the AeroStructures Test Wing¹ (ATW). The Dryden office had found a solution using linear aeroelastic analysis, but the result was incorrect and not conservative. The work on the nonlinear aeroelastic analysis stopped when problems developed with the CFD mesh. The model was then sent to the Computational AeroServoElasticity (CASE) Lab. The model included a completed surface description, boundary conditions, FEM structural model, and results from a ground vibrations test. The results of the CFD prediction would be compared the experimental tests. It was then intended to be a further validation of the *STARS*² suite for aeroservoelastic modeling.

The ATW was an 18-inch span carbon-fiber test wing. The ATW was flown on NASA Dryden's F-15B testbed. The wing made five flights. Each flight moved closer to the flutter point until the wing was initially brought to structural failure. The ground vibration test of the ATW is shown in figure 1.

The primary purpose of the ATW was to test the new *flutterometer*. The *flutterometer* is a software package designed to provide more data about the flutter characteristics of test structures. The sample is covered with actuators to read deflections during flight. These reading are used to predict the flutter boundary from experimental data.



Fig. 1, Ground Vibration Tests of the ATW

Methodology

This project was intended to validate the *STARS* suite and verify the new *Euler3d*³ codes for aeroelastic predictions. To accomplish this, the *STARS* suite uses both the *SOLIDS* structural dynamics solver code and a CFD flow solver.

Structural Model

The primary purpose of the structural solver in an aeroelastic case is to develop the structural mode shapes. This can be found from *SOLIDS* simulation of the structure or other sources, such as a ground vibration test. The output of the modes will be used later in the process as unsteady CFD runs are made.

The *STARS* system uses a FEM solver to find the free vibration response of the structure. This yields three important results. The first is the natural frequencies of the structure. These dictate the size of the time step needed during the CFD computations. It indicates which mode shapes are most important to flutter predictions, as high frequencies less likely to be excited than lower frequencies.

The second result that the FEM solver yields is the mode shapes themselves. The CFD solver

requires the deformation of the structure to find the aerodynamic loads. These forces are used to find the amplitude of the deflections for the next time step.

This is used by the third result from the structural solver, the dynamics system description. In reality, this system model is where the frequencies are determined. The model is based on a generalized displacement of the mode shapes. This allows the structural equations of motion to be expressed as simple ordinary differential equations. The system requires the input forces to solve the deflection and rate of change of the system.

Finite Element Mesh Generation

The first step in the CFD process is developing an accurate model of the structure's surface. This model must include the bounds of a surface, its overall shape and the direction of the vector normal to the surface.

The surfaces for the *STARS* suite are defined by their bounding curves. This sets the edge of the surface. Supporting surfaces are used to set the interior. For example the curve of a sphere must be defined, not just the circular outline. These interior support surfaces are used to find the vector normal to the surface directed into the flow.

Next, the density of the grid within the control volume and on the surfaces must be specified. Generally, areas suspected to have high gradients are discretized more heavily than the standard field. The leading and trailing edges wings are areas of severe gradients, so the grid density is set high in this region.

Boundary Conditions

With a complete grid, the *STARS* suite applies the boundary conditions. In this step the boundary condition for the surface are defined. The normal to the surface must be directed into the flow for *STARS* to apply the correct boundary conditions. Any areas where the surface normal is ambiguous are set as singularities. Listing a curve or surface as a singularity prevents the misapplication of the boundary conditions due to a vague normal definition.

Steady State Predictions

By this point the grid should be ready for use by the CFD solver. The input parameters need to be specified. These include the Mach number the angle of attack, side slide angle and various values relating to the method of solution. With these the steady state solution can be run. Normally the solution is run several times with increasing grid density. Once suitable grid spacing is found, the

steady state solution is considered an acceptable starting point for unsteady predictions.

Mode Shapes and Physical Parameters

Before unsteady runs can be made, the mode shapes must be transformed into an array of vectors that map to each node on the surfaces undergoing motion. The vectors indicate the strength and direction of the deflection caused by the mode shape. The relative strength to other deflections is most important. The absolute deflection due to any force will be found by multiplying the entire mode shape by a generalized displacement coefficient.

Results

The first goal of the project was to fix the errors occurring during the setting of the boundary conditions. This error manifested itself in the execution of the *setbnd2* program. After examining the error codes it was thought that the error was a problem with the surface definitions. Several surfaces were found to be defined with a normal vector directed out of the solver control volume, opposite of the correct direction. This problem was corrected by checking that all surfaces used a normal vector directed into the CFD control volume. The correction allowed the boundary conditions to be set.

The next task focused on developing the grid density needed to adequately capture the effects of the flow. The grid spacing following the wing was reduced to capture wake effects. The leading and trailing edges of the wing were treated as well. The overall grid spacing was reduced to generate a more refined grid. Solutions were run on three different grids to find one that produced an acceptable solution. The final grid selected is shown in figure 2.



Fig. 2a The wing surface

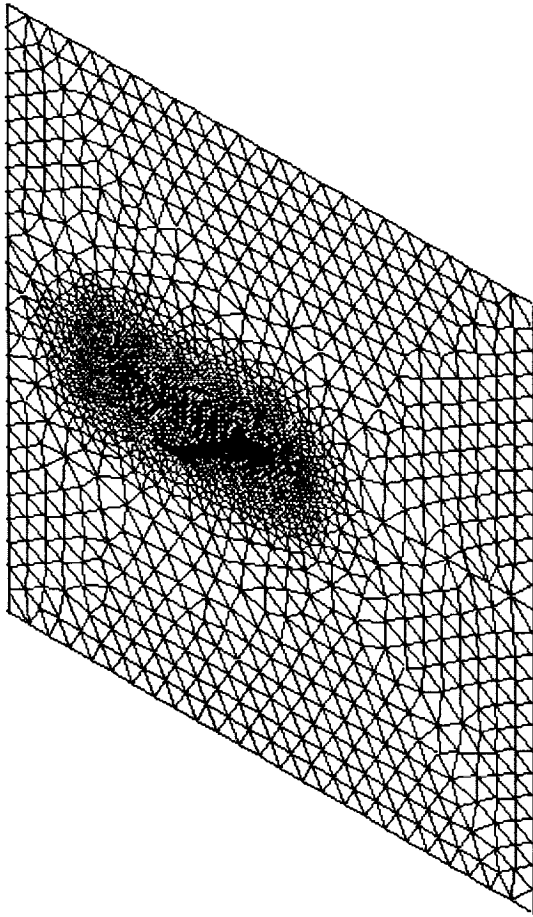


Fig. 2b The wing and surrounding mesh

This new grid required that the solids mode shape data be interpolated onto the CFD mesh. During this process, a new error occurred. Several grid points would have an interpolated normal deflection of zero. Although, only eight points were affected, this was thought to be a symptom of a larger problem. The *SOLIDS* model was investigated.

The *SOLIDS* structural model was a direct port of a *NASTRAN* model. This left several elements with little effect on the structural system in the model. These elements appear to affect the interpolating routines. The problem elements appeared to be the connections between the aileron and the wing structure. Since the aileron was glued in place, the aileron model and its connections to the wing were removed. It was replaced by solid wing elements that had properties similar to the elements around the aileron. The model also included elements within the wing that connected the wing rigidly to the wall. These elements served no purpose as the panel elements of the wing can have their initial and

boundary conditions set as pinned and clamped to the wall. These were removed as well. Figure 3 shows the FEM structural model and contains a brief description of changes made.

Three modes were assumed. The GVT data included only three modes and investigation of the higher mode showed their frequencies to be several times that of the first mode. The first mode was a primarily bending deflection. The second mode was torsional. The third was dominated by bending, but contain noticeable amount of twist.

The model of the structure was compared to both the direct *NASTRAN* port and the Ground Vibration Test results. The natural frequencies of each of the modes are listed in table 1. The deflection in the vertical direction is compared in figure 4a-c for all three modes. The figure contains a cross sectional (chord-wise) cut of the deflections. The GVT data is considered the base line and the *SOLIDS* model should be as close as possible. The reduction of elements improved the model. This is most evident in mode 2, the first torsion mode. The interpolation of the structural modes onto the grid mesh is shown in figure 5a-c.

	Mode 1	Mode 2	Mode 3
GVT	14.5 Hz	23.3 Hz	84.65 Hz
<i>NASTRAN</i> -port	14.8 Hz	21.5 Hz	94.76 Hz
New Simplified	15.0 Hz	21.8 Hz	95.86 Hz

Table 1 Comparison of the frequencies of the GVT and two variant *SOLIDS* input models

The steady solution to the grid was compared to the unsteady solution with all modes held rigidly in their zero displacement orientation. The solutions match, as a cross sectional pressure plot for both steady and unsteady yielded identical results.

Once the mode shapes were found an unsteady state solution could be developed. The unsteady solver of *STARS* fails when attempting to find a solution to the ATW simulation. It is believed that this problem may be corrected by increasing grid density aft of the boom. However, *Euler3d* does not have this problem. It does find does a steady and unsteady solution for the ATW grid. The results listed here are from the *Euler3d* codes. The steady and unsteady solutions are compared in figure 6. The unsteady is a free response after reaching steady state.

Conclusions

The changes to the surface definition have fixed the errors due to misdefinition of the normal vectors. The simplification of the structural inputs

has not reduced the accuracy of the structural model. Currently, work is proceeding on determining the location of the flutter boundary.

References

¹Potter, Star, Lind, Rick, "Developing Uncertainty Models for Robust Flutter Analysis

Using Ground Vibration Test Data", NASA TM-2001-210392, 2001.

²Gupta, K. K., "STARS-An Integrated, Multidisciplinary, Finite-Element, Structural, fluids, Aeroelastic, and Aeroservoelastic Analysis Computer Program", NASA TM-4795, 1997.

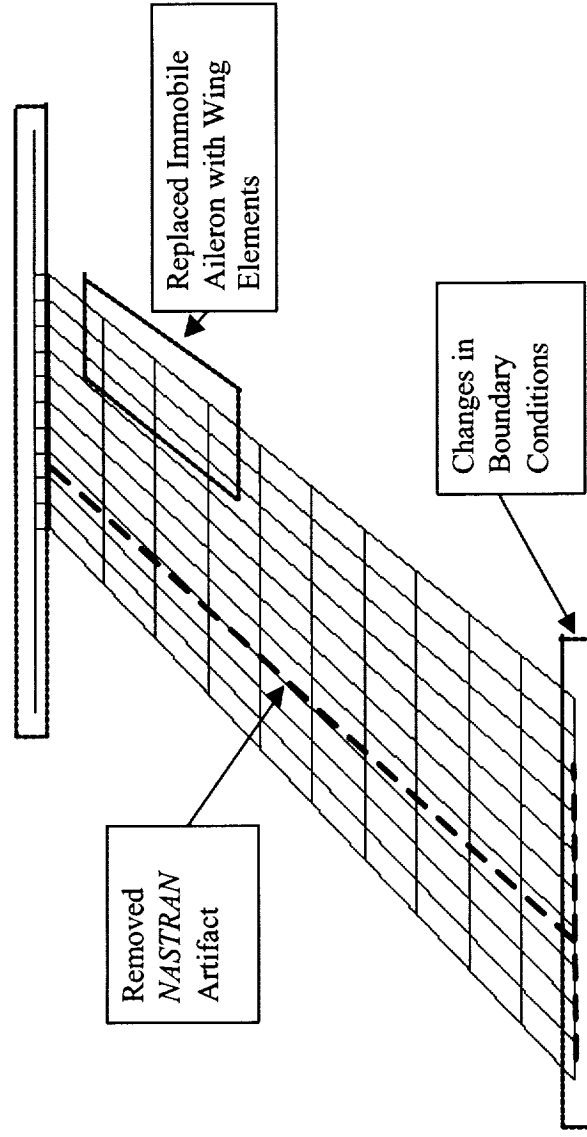


Fig. 3 The ATW Structural model. The aileron model was removed and replaced with plat elements. An odd set of elements enforcing the boundary conditions was removed, and the nodes at the wall set to the correct boundary conditions.

**Mode 1
80% Span**

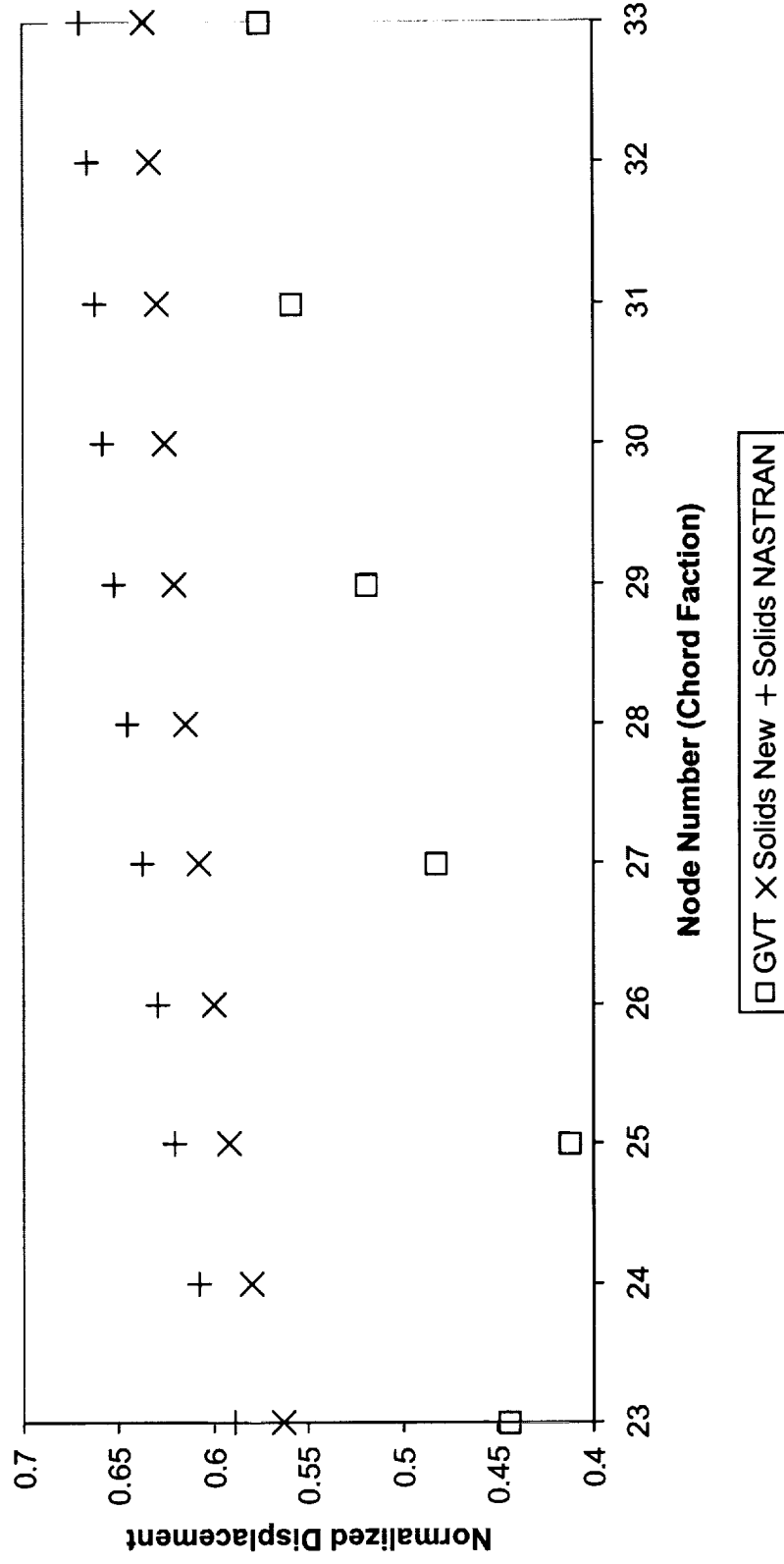


Fig. 4 a The vertical deflection at nodal points. This is a chordwise cut at 80% span of the ATW. The deflections have been normalized for comparison. The node number start at 23, the leading edge, and continue to 33, the trailing edge.

Mode 2 80% Span

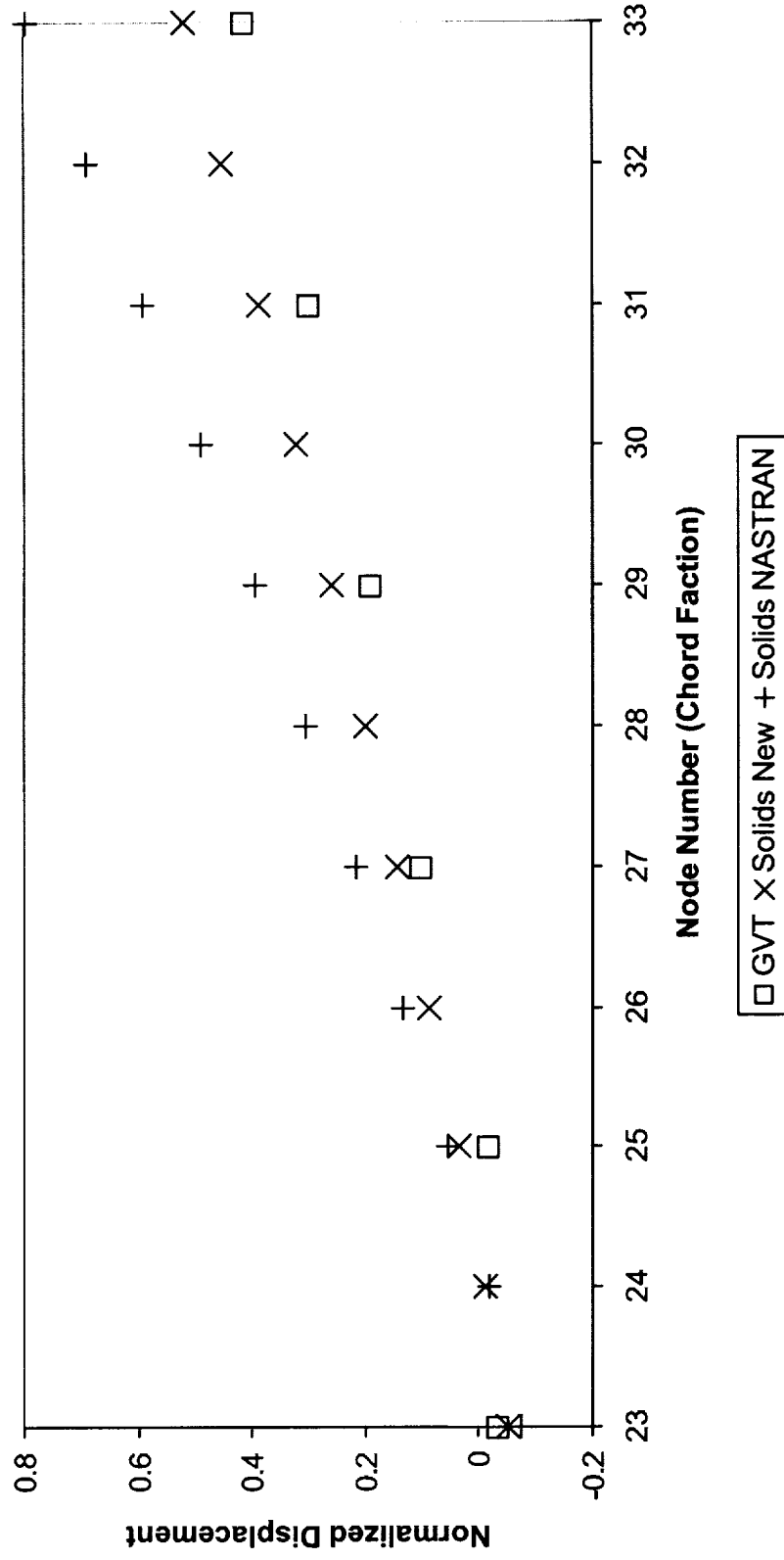


Fig. 4b The vertical deflection at nodal points. This is a chordwise cut at 80% span of the A.T.W. The deflections have been normalized for comparison. The node number start at 23, the leading edge, and continue to 33, the trailing edge.

Mode 3 80% Span

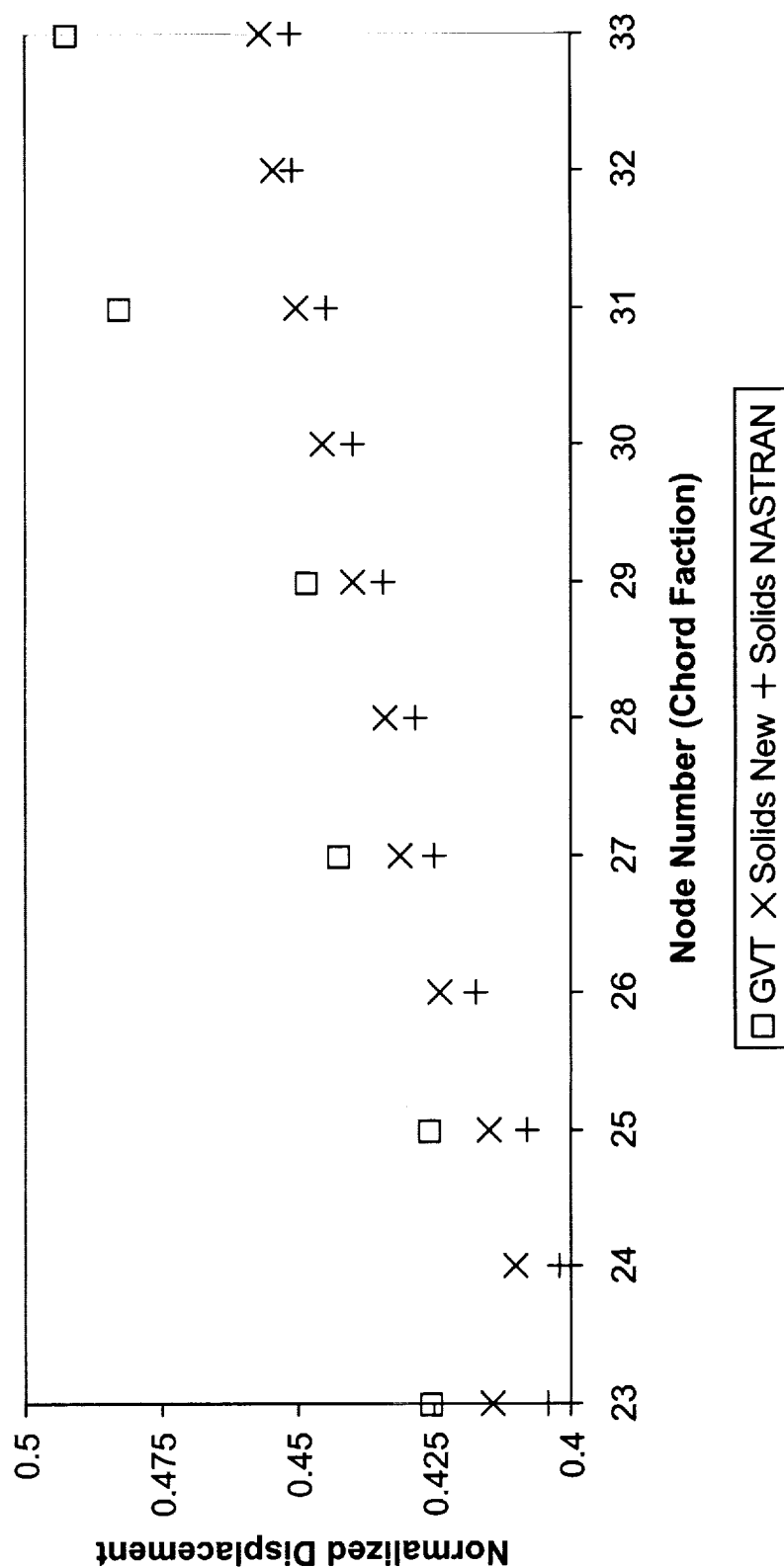


Fig. 4c The vertical deflection at nodal points. This is a chordwise cut at 80% span of the ATW. The deflections have been normalized for comparison. The node number start at 23, the leading edge, and continue to 33, the trailing edge.

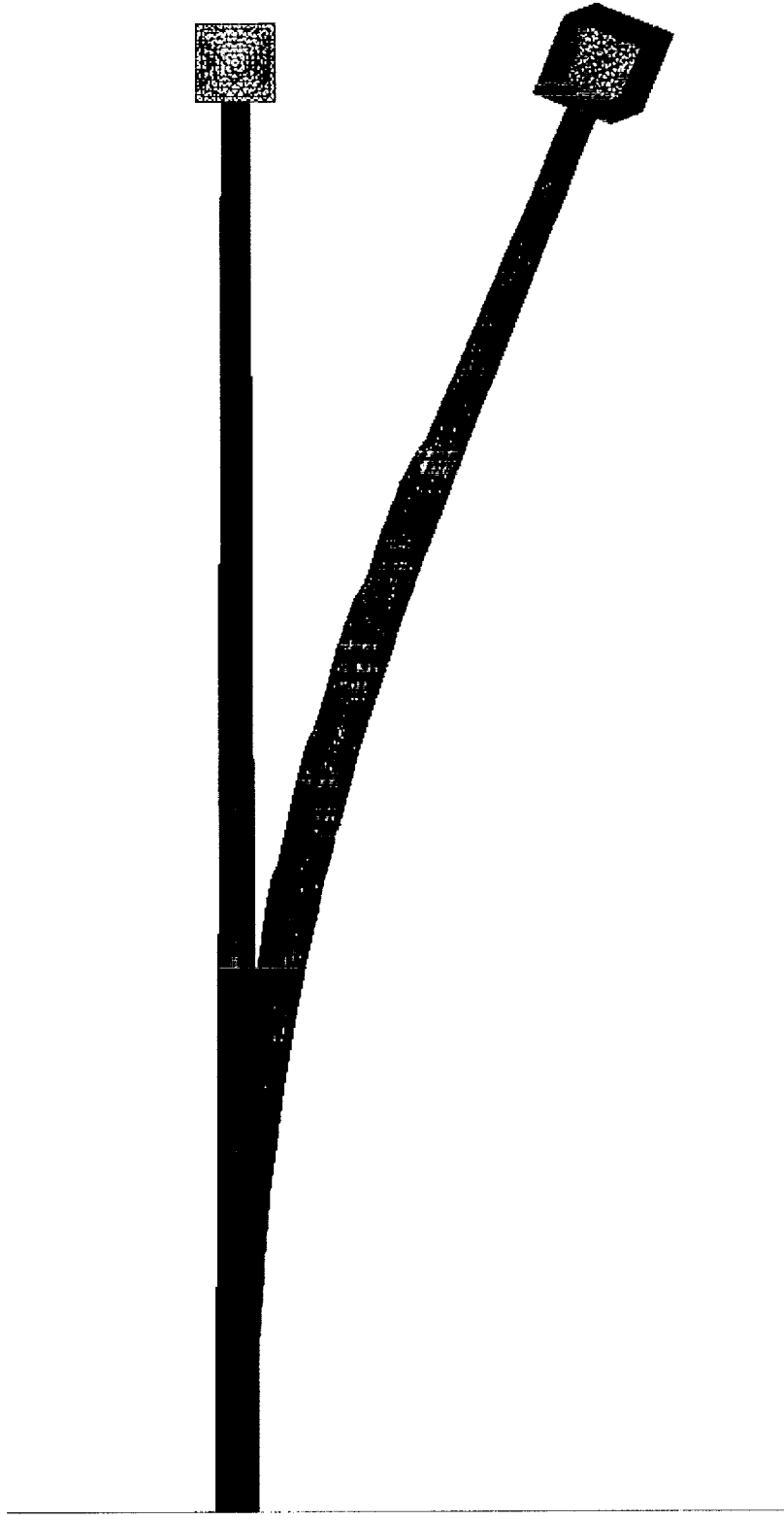


Fig. 5a Mode 1, First Bending, 15 Hz

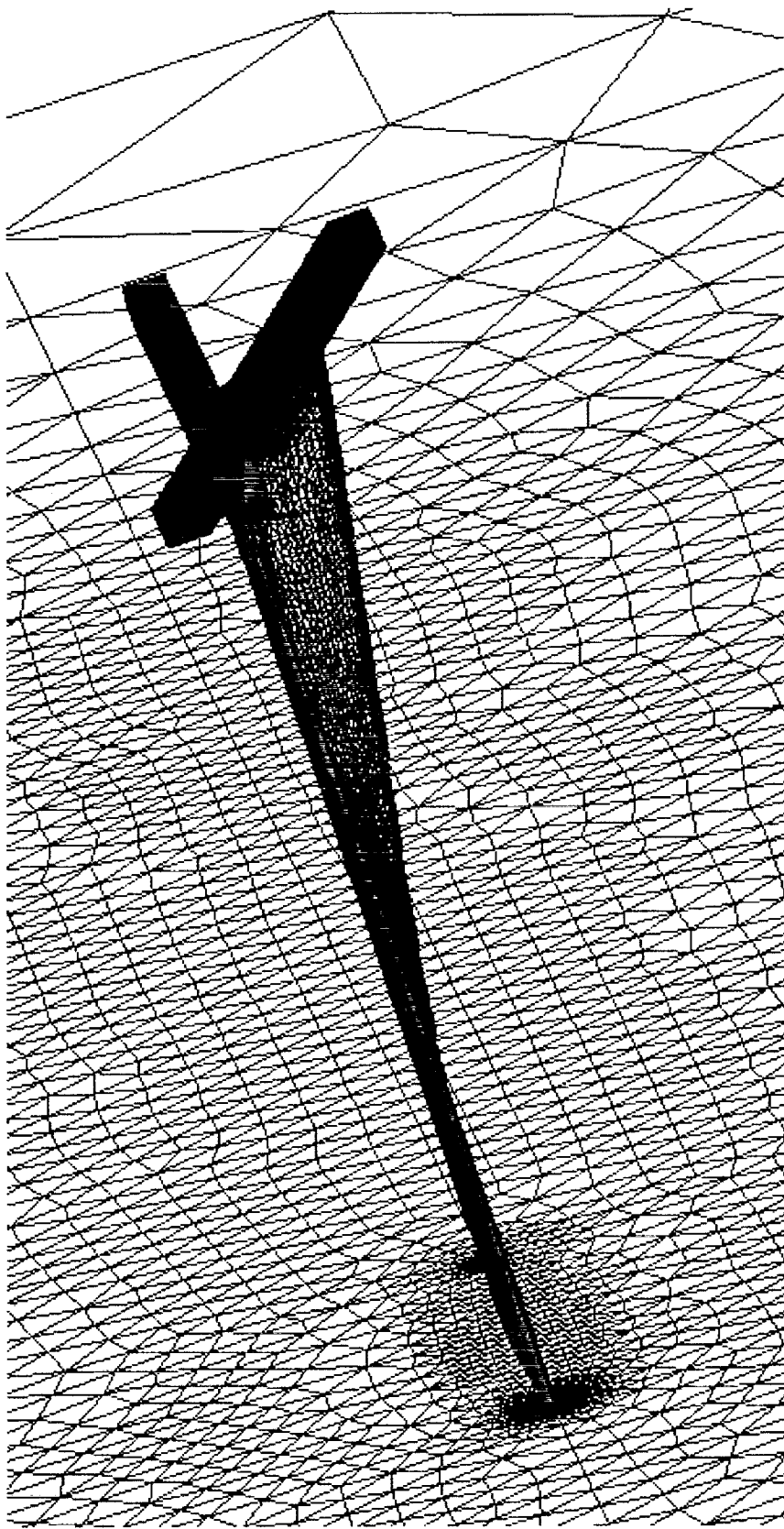


Fig. 5b Mode 2, First Torsion, 22 Hz

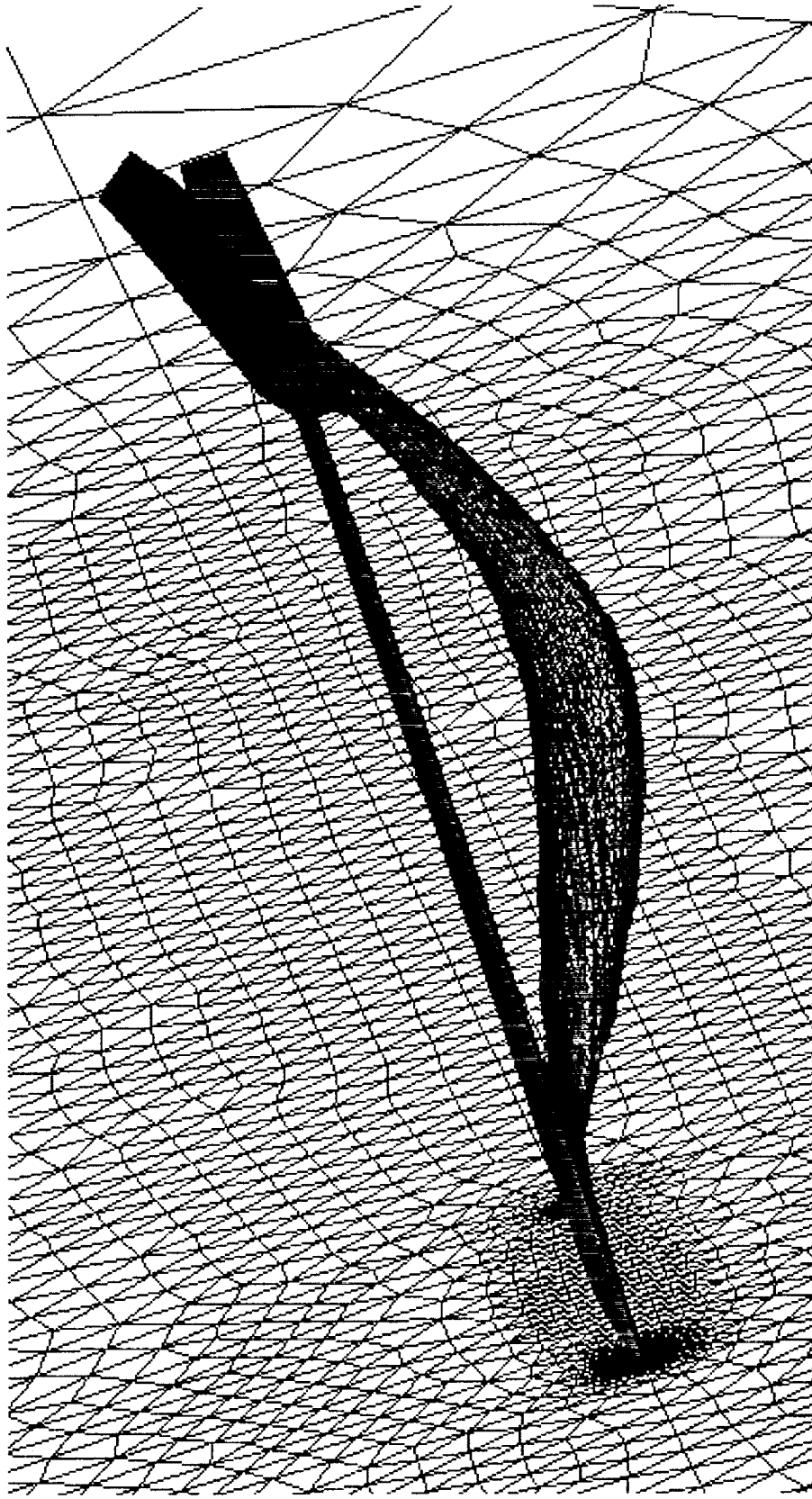


Fig. 5c Mode 3, Second Bending, 95 Hz

C_p Plot of ATW

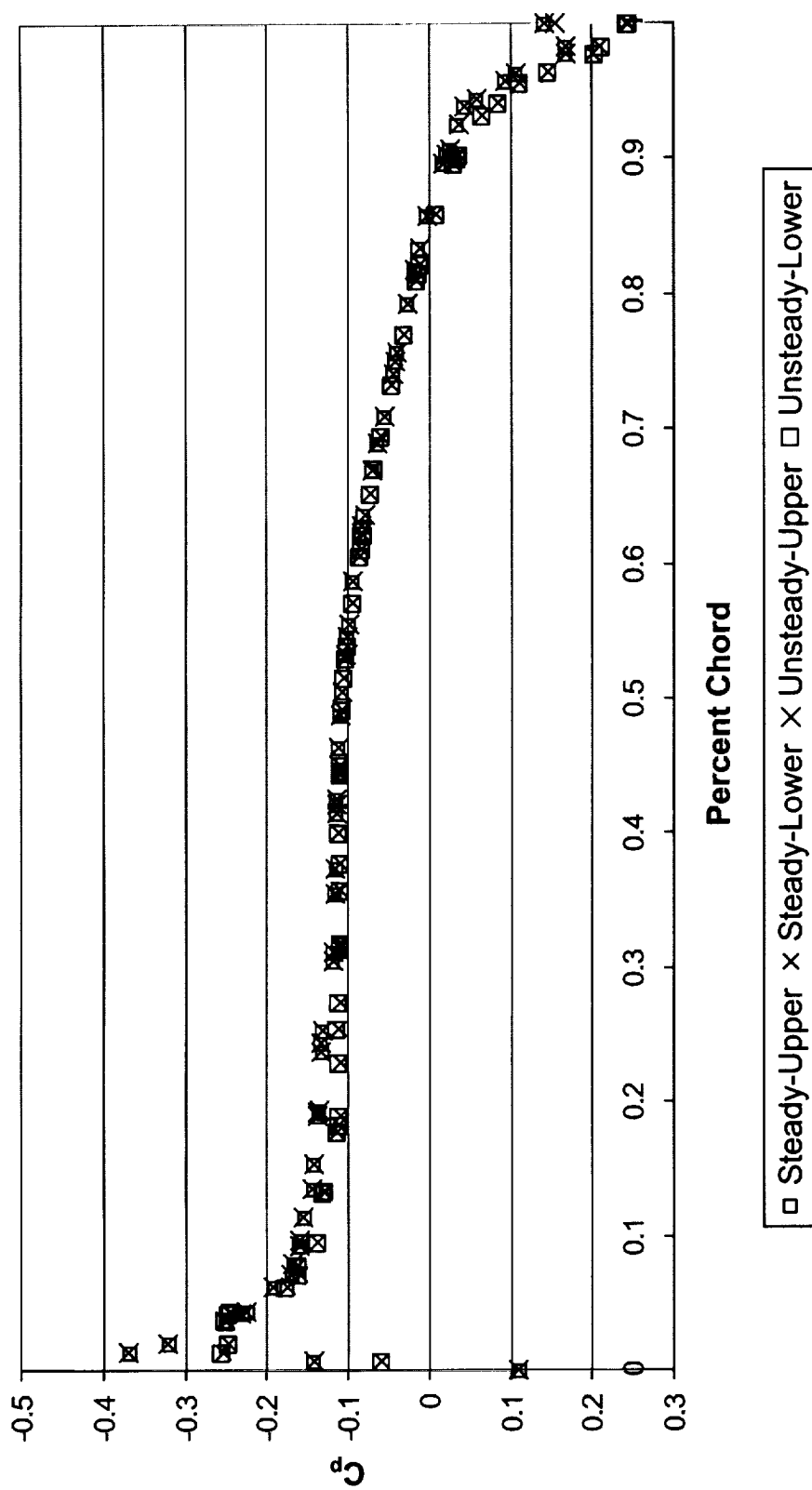


Fig. 6 A comparison of the steady and unsteady with rigidly held modes. The values are identical. The steady and unsteady solution solvers agree.